Molecular Therapy
Original Article

# miR-491 Inhibits Osteosarcoma Lung Metastasis and Chemoresistance by Targeting αB-crystallin

Shu-Nan Wang,[1,10] Song Luo,[2,10] Chang Liu,[3] Zhenghao Piao,[4] Wenlong Gou,[5] Yun Wang,[6] Wei Guan,[7] Qing Li,[7] Hua Zou,[7] Zhen-Zhou Yang,[7] Dong Wang,[7] Yan Wang,[2] Meng Xu,[2] Hua Jin,[8,9] and Cheng-Xiong Xu[7]

[1]Department of Radiology, Daping Hospital and Research Institute of Surgery, Third Military Medical University, Chongqing 400042, China; [2]Department of Orthopaedics, The General Hospital of Chinese People's Liberation Army, Beijing 100853, China; [3]Department of Biochemistry and Molecular Biology, School of Basic Medical Sciences, Jilin University, Changchun 130021, China; [4]Department of Basic Medical Science, School of Medicine, Hangzhou Normal University, Hangzhou 310036, China; [5]Department of Orthopaedics, Daping Hospital and Research Institute of Surgery, Third Military Medical University, Chongqing 400042, China; [6]Department of Pathology, The General Hospital of Chinese People's Liberation Army, Beijing 100853, China; [7]Cancer Center, Daping Hospital and Research Institute of Surgery, Third Military Medical University, Chongqing 400042, China; [8]Department of Thoracic Surgery, Daping Hospital and Research Institute of Surgery, Third Military Medical University, Chongqing 400042, China; [9]Department of Pharmaceutical Science, College of Pharmacy, University of South Florida, Tampa, FL 33612, USA

**Dysregulated microRNAs (miRNAs) play an important role in osteosarcoma (OS) progression. In the present study, we investigate the clinical significance of serum miR-491 level and the potential role of miR-491 in OS lung metastasis and chemoresistance. Clinical data show that the level of miR-491 was decreased in serum from OS patients compared with healthy control subjects, and that a decreased serum miR-491 level is correlated with increased metastasis, poor chemoresponse, and lower survival rate in OS patients. In vitro and in vivo experiments show that overexpression of miR-491 suppresses OS cell lung metastasis, whereas it enhances cisplatin (CDDP)-induced tumor growth inhibition and apoptosis. In contrast, inhibition of miR-491 stimulates OS cell lung metastasis and suppresses CDDP-induced tumor growth inhibition and apoptosis. Furthermore, we demonstrate that miR-491 exerts its role by directly targeting αB-crystallin (CRYAB) in OS. Our findings suggest that serum level of miR-491 has potential as a biomarker for predicting OS progression and prognosis of OS patients. Additionally, restoration of miR-491 may be a novel strategy for inhibiting OS lung metastasis and overcoming OS cell resistance to chemotherapy.**

## INTRODUCTION

Osteosarcoma (OS) is the most common primary malignant tumor in children and adolescents.[1] The standard care for OS patients leads to an overall 5-year survival rate of approximately 70%.[2] However, 30% of patients diagnosed with OS will not survive for more than 5 years, and fewer than 50% will live beyond 10 years.[3–5] Treatment of OS often fails because of the development of chemoresistance and metastasis.[5,6] However, there are no predictive biomarkers or effective treatment methods for OS metastasis and chemoresistance. Thus, a comprehensive understanding of OS biology is required to optimize treatment strategies and to develop new therapeutic agents for OS patients with metastasis or chemoresistance. However, the cellular mechanisms that lead to the development of OS chemoresistance and metastasis remain unclear.

αB-crystallin (CRYAB) is a human small heat shock protein and is involved in cancer progression. Recent studies show that CRYAB was upregulated in several types of human cancers including hepatocellular carcinoma,[7] breast cancer,[8] and OS.[9] In addition, studies show that increased expression of CRYAB was closely related with cancer metastasis, chemoresistance, and poor prognosis in OS patients,[9,10] indicating that CRYAB plays an oncogenic role in OS. However, the mechanism by which the CRYAB expression is upregulated in cancer is largely unknown.

MicroRNAs (miRNAs) are a family of small, noncoding RNA molecules that play important roles in many normal biological processes, including cell proliferation, differentiation, and apoptosis and organ development.[11,12] miRNAs function by negatively regulating gene expression through direct binding to the 3′ UTR of a target gene mRNA, which induces mRNA cleavage or translational repression.[11,12] Interestingly, accumulating evidence suggests that certain miRNAs undergo aberrant regulation during carcinogenesis, chemoresistance, and metastasis in many cancers, including OS.[13–17] More importantly, studies have shown that restoration or inhibition of these aberrantly regulated miRNAs can dramatically suppress cancer progression, indicating that miRNAs can be developed as effective therapeutic agents or targets for cancer treatment.[15–17] Additionally, clinical evidence shows that miRNAs may become fantastic diagnostic and/or prognostic biomarkers in cancers.[18] For example, serum miR-200c has been identified as a biomarker of relapse in stage

Received 12 January 2017; accepted 25 May 2017;
http://dx.doi.org/10.1016/j.ymthe.2017.05.018.

[10]These authors contributed equally to this work.

**Correspondence:** Cheng-Xiong Xu, Cancer Center, Daping Hospital and Research Institute of Surgery, Third Military Medical University, Chongqing 400042, China.
**E-mail:** xuchengxiong@hanmail.net
**Correspondence:** Hua Jin, Department of Thoracic Surgery, Daping Hospital and Research Institute of Surgery, Third Military Medical University, Chongqing 400042, China.
**E-mail:** jinhua12001@hanamil.net

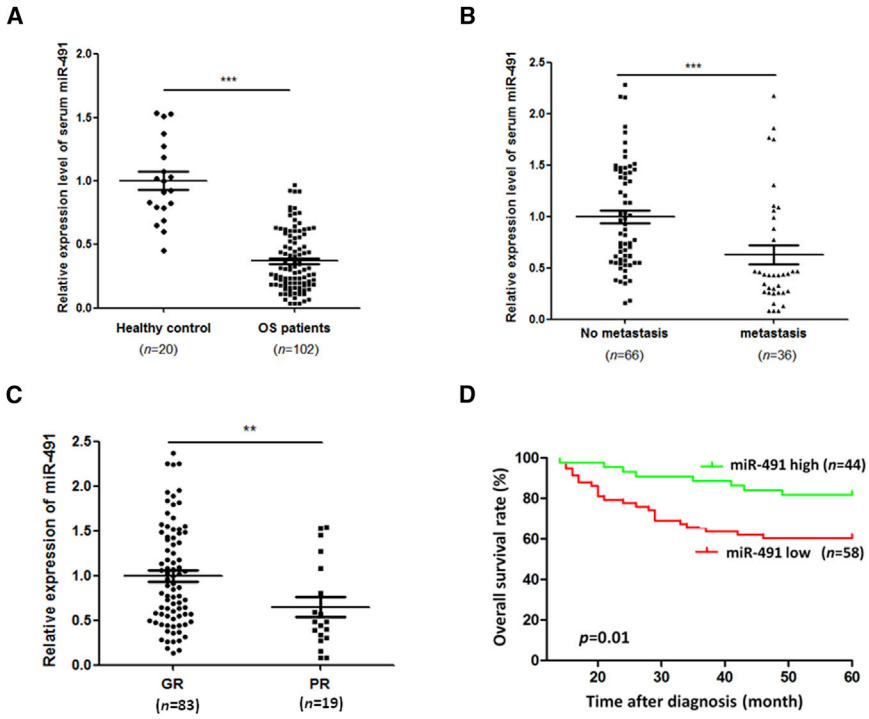


**Figure 1. Downregulated Expression Level of miR-491 in Serum Was Correlated with OS Progression**

(A) The level of serum miR-491 was significantly decreased in OS patients (n = 102) compared with healthy control subjects (n = 20). (B) The level of serum miR-491 was significantly decreased in OS patients with metastasis (no metastasis) (n = 36) compared with patients with no metastasis (metastasis) (n = 66). (C) The level of serum miR-491 was significantly decreased in OS patients with poor chemoresponse (PR) (n = 19) compared with those with a good chemoresponse (GR) (n = 83). The level of miR-491 in serum was measured by qRT-PCR. (D) Kaplan-Meier analysis of overall survival rate for patients with OS with low and high serum miR-491 levels. *p < 0.05; **p < 0.01; ***p < 0.001.

l epithelial ovarian cancer,[19] and serum miR-1290 has been identified as a biomarker for early detection, recurrence, and prognosis in colorectal cancer.[20]

Downregulated expression of miR-491 was identified in several cancer tissues compared with normal tissues, including OS.[21,22] However, the clinical significance of the serum level of miR-491 and the detailed mechanisms of its involvement in OS progression still remain to be fully clarified. Here, we determined that level of serum miR-491 was indeed downregulated in OS patients compared with healthy controls, and downregulated miR-491 in serum was closely correlated with increased metastasis, poor chemoresponse, and low overall survival in patients with OS. Our data indicate that miR-491 is a tumor-suppressor miRNA that inhibits OS growth and OS cell lung metastasis, and enhances the sensitivity of OS cells to cisplatin (CDDP) treatment. In addition, we demonstrate that miR-491 exerts its tumor-suppressing activity by directly targeting CRYAB in OS.

## RESULTS

### Decreased Level of Serum miR-491 Was Closely Correlated with Worse Clinical Outcomes in OS Patients

To investigate whether the serum miR-491 expression levels were different between OS patients and healthy subjects, we first measured the level of miR-491 in serum from 102 newly diagnosed OS patients (no metastasis at diagnosis) and 20 healthy control subjects by qRT-PCR. As shown in Figure 1A, the level of serum miR-491 was significantly decreased in OS patients compared with healthy controls. Then, to investigate the clinical significance of the serum miR-491 level in OS, we divided the 102 OS patients into high- and low-miR-491 expression groups based on the mean level of miR-491 in OS patient serum, and patients were followed up. As shown in Table 1, our follow-up data indicate that the OS patient group with the low level of serum miR-491 had a higher metastatic rate and poorer chemoresponse compared with the high-level serum miR-491 OS patient group. Consistent with these follow-up data, our qRT-PCR results show that OS patients with metastasis or a poor chemoresponse present lower serum miR-491 compared with OS patients with no metastasis or a good chemoresponse (Figures 1B and 1C). In addition, our Kaplan-Meier survival analysis demonstrates that the OS patient group with the low level of serum miR-491 had a lower overall survival rate compared with the OS patient group with a high level of serum miR-491 (Figure 1D). Importantly, multivariable analyses show that miR-491 is an independent predictor of OS patients' prognosis (Table 2). Taken together, these results suggest that decreased expression of miR-491 indicates a poor prognosis and may be involved in the stimulation of OS metastasis and chemoresistance.

### Inhibition of miR-491 Stimulates OS Cell Lung Metastasis and Chemoresistance Both In Vitro and In Vivo

Next, we investigated whether decreased expression of miR-491 was involved in OS cell lung metastasis and chemoresistance in several OS cell lines by inhibiting miR-491 (Figures S1A and S1B). As shown in Figure 2A, in vitro Transwell assays indicate that inhibition of miR-491 can significantly promote OS cell invasion in both U2OS and Saos-2 cells. In addition, western blot analysis shows that inhibition of miR-491 reduced anti-metastatic protein E-cadherin expression and increased pro-metastatic protein MMP-9 expression in OS cells (Figure 2B). Furthermore, we use animal models to investigate whether inhibition of miR-491 could induce similar effects on metastasis in vivo. 143B cells that express miR-491-antisense were injected into the intramedullar cavity of the tibia, and mice were sacrificed 4 weeks after cell injection. Data show that

**Table 1. Correlation of Serum miR-491 Level and Chemotherapy Response and Metastasis in OS Patients**

| | No. of Patients (%) | | |
|---|---|---|---|
| | miR-491 Low | miR-491 High | p Value |
| Response to Chemotherapy | | | |
| Good response | 41 (70.69) | 42 (95.45) | 0.001 |
| Poor response | 17 (29.31) | 2 (4.55) | 0.001 |
| Metastasis | | | |
| Yes | 26 (44.83) | 10 (22.73) | 0.023 |
| No | 32 (54.17) | 34 (77.27) | 0.023 |

**Table 2. Univariate and Multivariable Analyses of Factors Predictive of Poor Overall Survival in OS Patients**

| | Univariate Analysis | | Multivariate Analysis | |
|---|---|---|---|---|
| Variable | HR (95% CI) | p Value | HR (95% CI) | p Value |
| Gender | 1.32 (0.62–2.81) | 0.47 | 2.96 (0.70–3.95) | 0.25 |
| Age | 1.00 (0.95–1.04) | 0.69 | 0.97 (0.92–1.02) | 0.18 |
| Anatomical site | | 0.78 | | 0.39 |
| Histologic subtype | | 0.76 | | 0.13 |
| Histologic grade | 1.71 (0.59–4.96) | 0.32 | 1.11 (0.34–3.62) | 0.87 |
| Enneking grade | 1.89 (0.76–4.69) | 0.17 | 1.72 (0.61–4.85) | 0.30 |
| miR-491 level | 3.15 (1.27–7.81) | 0.01 | 2.96 (1.09–8.07) | 0.03 |
| Response to chemotherapy | 0.23 (0.11–0.50) | <0.01 | 0.11 (0.04–0.29) | <0.01 |

CI, confidence interval; HR, hazard ratio.

inhibition of miR-491 (Figure S1C) stimulated 143B cell lung metastasis compared with vector control (Figure 2C); these results were confirmed using other OS lung metastatic models. MG63 or Saos-2 cells that stably expressed miR-491-antisense (Figures S1D and S1E) were injected into nude mice through the tail vein. These mice were sacrificed 6 weeks after injection, and the lung surface tumor nodules were counted. The results show that inhibition of miR-491 significantly increased OS cell lung metastasis compared with the vector control groups in both MG63 and Saos-2 cell lung metastasis models (Figure S2A). Additionally, we examined the effects of miR-491 inhibition on the chemotherapeutic sensitivity of OS cells. As shown in Figures 2D and 2E, 3-(4,5-dimethylthiazol-2-yl)-2, 5-diphenyltetrazolium bromide (MTT) and apoptosis assays show that inhibition of miR-491 can protect cells from CDDP-induced cell death in both U2OS and Saos-2 cells. Consistent with these results obtained from in vitro experiments, the inhibition of miR-491 significantly suppressed CDDP-induced tumor growth inhibition and apoptosis in MG63 (Figures 2F and 2G) and Saos-2 xenograft models (Figures S2B and S2C). Inhibition of miR-491 also stimulated cell proliferation compared with the vector control group and suppressed CDDP-induced tumor cell proliferation inhibition (Figure 2H). Taken together, these findings suggest that decreased expression of miR-491 in OS significantly contributes to tumor metastasis and chemoresistance.

### Overexpression of miR-491 Inhibits OS Cell Lung Metastasis and Chemoresistance

Our observations that inhibition of miR-491 stimulates OS cell lung metastasis and chemoresistance in turn prompted us to investigate whether miR-491 overexpression could suppress OS cell lung metastasis and chemoresistance. As shown in Figures 3A–3C, our in vitro results clearly show that overexpression of miR-491 can significantly inhibit OS cell invasion (Figure 3A) and the expression of pro-metastatic protein MMP-9 increased anti-metastatic protein E-cadherin expression in both U2OS and Saos-2 cells (Figure 3B). In addition, overexpression of miR-491 enhances CDDP-induced cell growth inhibition and apoptosis in both U2OS and Saos-2 cells (Figures 3C and 3D). These results were further confirmed using animal models. Consistent with the in vitro experiments, the in vivo results showed that overexpression of miR-491 dramatically suppressed OS cell lung metastasis (Figure 3E; Figure S2D) and enhanced CDDP-induced tumor growth inhibition, proliferation, and apoptosis compared with the control group in OS cell xenograft models (Figures 3F–3H; Figures S2E and S2F). Taken together, these data suggest that restoration of miR-491 may be a novel strategy for treatment of OS lung metastasis and chemoresistance.

### miR-491 Inhibits OS Lung Metastasis and Chemoresistance through Direct Targeting of CRYAB

To investigate the underlying mechanism of the effect of miR-491 on OS cell metastasis and chemoresistance, we used miRNA target prediction algorithms (http://targetscan.org and http://microrna.org) to screen miR-491 target genes, and we identified CRYAB as a tentative target of miR-491 (Figure 4A), because a previous report shows that CRYAB is highly expressed in human OS tissues and is closely correlated with OS progression.[9] To investigate the association between miR-491 and CRYAB expression, we examined the expression level of CRYAB in miR-491-overexpressing or miR-491-inhibited OS cells. As shown in Figure 4B, the expression of CRYAB was significantly decreased in miR-491-overexpressing MG63 cells at both the mRNA and protein levels compared with control cells. In contrast, inhibition of miR-491 led to an increase in the expression of CRYAB at both the mRNA and the protein level (Figure 4B). Also, the miR-491 negatively regulates CRYAB downstream of signal or protein expression, including ERK signaling and MMP-9 expression (Figure 4B). Next, to determine whether the regulation of CRYAB-luciferase expression depends on the binding of their complementary 3′ UTR sequences to the miR-491 seed sequence, we inserted a 3-nt mutation into the CRYAB 3′ UTR, as indicated in Figure 4A. Our data show that overexpression of miR-491 significantly repressed the luciferase activity associated with the wild-type 3′ UTR. In contrast, the 3′ UTR mutation completely abrogated the effect of miR-491 overexpression on luciferase activity in MG63 cells (Figure 4C). Furthermore, we investigated the correlation between miR-491 and CRYAB expression in human OS specimens. Data show that the expression of

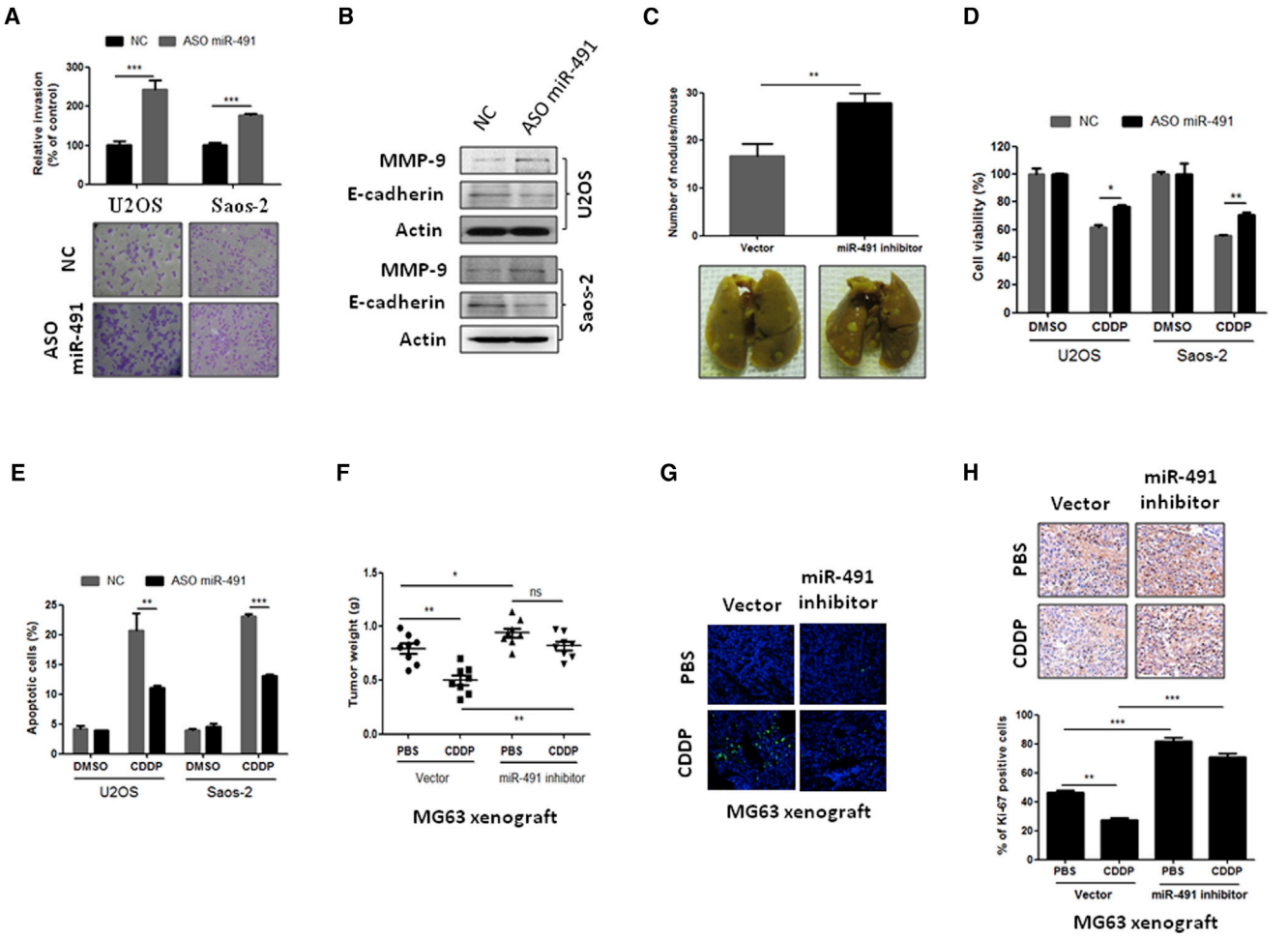


**Figure 2. Inhibition of miR-491 Stimulates OS Metastasis and Chemoresistance In Vitro and In Vivo**

(A) Inhibition of miR-491 stimulated OS cell invasion in both U2OS and Saos-2 cells. Cells were transfected with negative control oligonucleotides (NC) or antisense oligonucleotides of miR-491 (ASO miR-491). After 24 hr of transfection, cells were subjected to an invasion assay. (B) Inhibition of miR-491 reduced E-cadherin expression and increased MMP-9 expression in OS cells. Indicated cells were transfected with NC or ASO miR-491. After 72 hr of transfection, cells were subjected to western blot analysis. (C) Inhibition of miR-491 stimulates OS lung metastasis in vivo. 143B cells were transfected with miR-491-antisense oligonucleotides expressing plasmid or empty vector. After 48 hr of transfection, cells were injected into the intramedullary cavity of the tibia of 6-week-old nude mice (n = 5 per group). The mice were sacrificed 4 weeks after cell injection, and the lung surface nodules were counted under microscopy. (D) Inhibition of miR-491 suppressed CDDP-induced cell growth inhibition in both U2OS and Saos-2 cells. After 24 hr of transfection with the indicated oligonucleotides, cells were plated into a 96-well plate. 12 hr after seeding, cells were incubated with or without CDDP (10 μM) for 48 hr and then subjected to an MTT assay. (E) Inhibition of miR-491 attenuated CDDP-induced apoptosis in U2OS and Saos-2 cells. 24 after transfection with the indicated oligonucleotides, cells were plated into a six-well plate. After 12 hr of seeding, cells were incubated with or without CDDP (10 μM) for 24 hr and then subjected to a flow cytometry assay. (F) Inhibition of miR-491 promotes tumor growth and induces resistance to CDDP in MG63 xenograft models. Stably expressing miR-491-antisense cells were injected subcutaneously into nude mice (n = 8 per group). After the tumor size reached approximately 100 $mm^3$, the mice were started on a treatment of either PBS or CDDP (10 mg/kg body weight). The mice were sacrificed after 3 weeks of CDDP treatment, and the tumor weight was measured. (G) Apoptotic cells were detected using a TUNEL assay in the indicated xenograft tumor samples. (H) Inhibition of miR-491 promotes cancer cell proliferation in MG63 xenograft models. Tumor tissues from the MG63 xenograft model were stained with Ki-67. *$p < 0.05$; **$p < 0.01$; ***$p < 0.001$.

miR-491 was inversely correlated with CRYAB expression in OS patient specimens (Figure 4D). Cumulatively, these data suggest that miR-491 negatively regulates the expression of CRYAB by directly targeting its 3′ UTR sequence.

We also investigated the correlation between forkhead box P4 (FOXP4) and miR-491 in OS specimens, because this protein has been reported to be regulated by miR-491 in OS cells.[21] However, our data show that miR-491 and FOXP4 expression are not inversely correlated in OS specimens (Figure S3), suggesting that FOXP4 is not a major target gene of miR-491 in OS.

Further, to determine whether CRYAB directly contributes to miR-491 function, we overexpressed CRYAB in miR-491-overexpressing

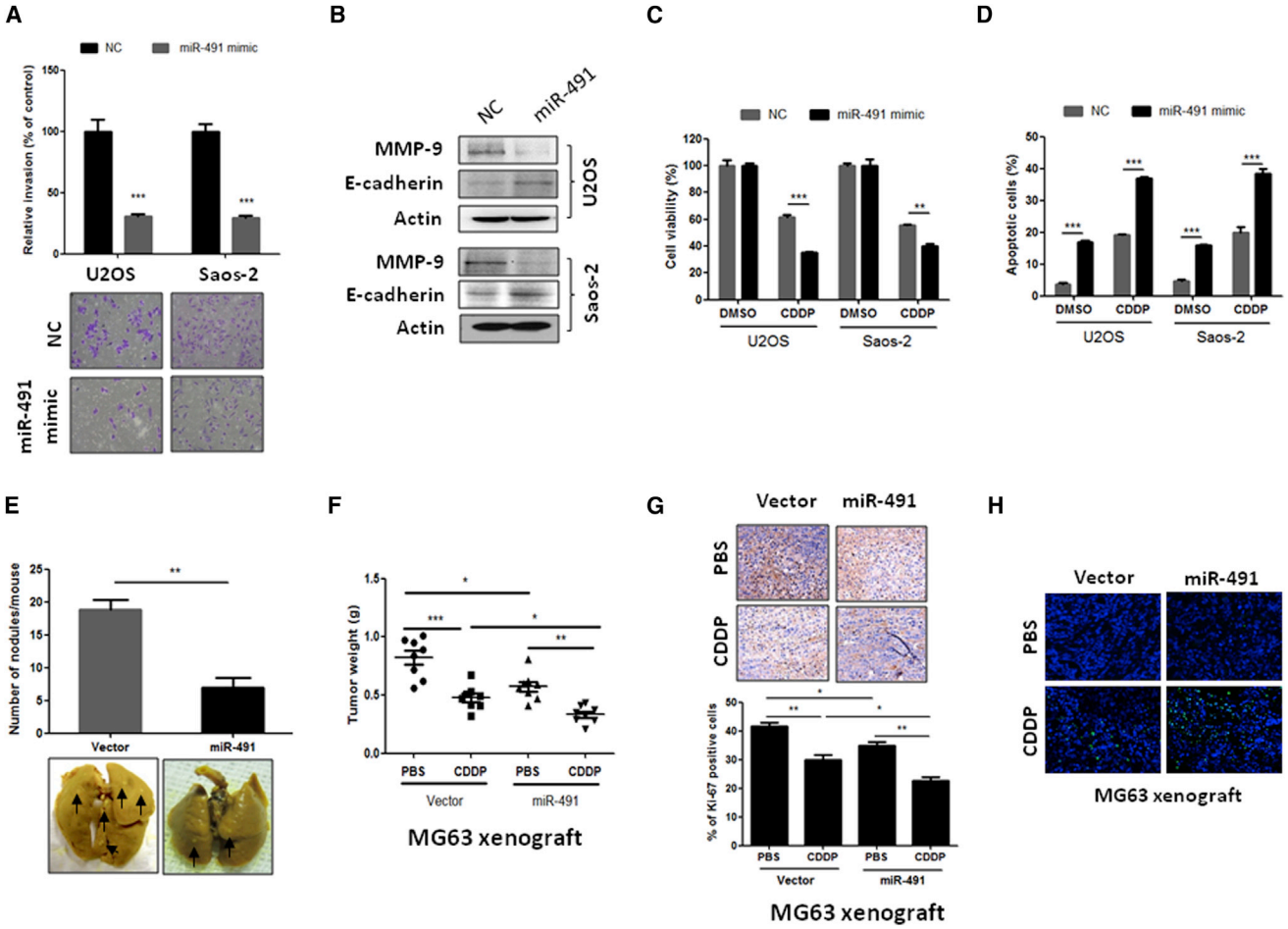


**Figure 3. Overexpression of miR-491 Inhibits OS Metastasis and Enhances Chemosensitivity In Vitro and In Vivo**

(A) Overexpression of miR-491 inhibited OS cell invasion in both U2OS and Saos-2 cells. Cells were transfected with negative control oligonucleotides (NC) or miR-491 mimics. After 24 hr of transfection, cells were subjected to an invasion assay. (B) Overexpression of miR-491 increased E-cadherin expression and reduced MMP-9 expression in OS cells. Indicated cells were transfected with NC or miR-491 mimics. After 72 hr of transfection, cells were subjected to western blot analysis. (C) Overexpression of miR-491 enhanced CDDP-induced cell growth inhibition in both U2OS and Saos-2 cells. After 24 hr of transfection with the indicated oligonucleotides, cells were plated into a 96-well plate. 12 hr after of seeding, cells were incubated with or without CDDP (10 μM) for 48 hr and subjected to an MTT assay. (D) Overexpression of miR-491 enhanced the CDDP-induced apoptosis in both U2OS and Saos-2 cells. After 24 hr of transfection with the indicated oligonucleotides, cells were plated into a six-well plate. 12 hr after of seeding, cells were incubated with or without CDDP (10 μM) for 24 hr and then subjected to a flow cytometry assay. (E) Overexpression of miR-491 inhibits OS lung metastasis in vivo. 143B cells were transfected with miR-491 expression plasmid or empty vector. After 48 hr of transfection, cells were injected into the intramedullary cavity of the tibia of 6-week-old nude mice (n = 5 per group). The mice were sacrificed 4 weeks after cell injection, and the lung surface nodules were counted under microscopy. (F) Overexpression of miR-491 inhibits tumor growth and enhances CDDP-induced tumor growth inhibition in a xenograft model. Stably expressing miR-491 MG63 cells were injected subcutaneously into nude mice (n = 8 per group). After the tumor size reached approximately 100 $mm^3$, the mice were started on a treatment of either PBS or CDDP (10 mg/kg body weight). The mice were sacrificed after 3 weeks of CDDP treatment, and the tumor weight was measured. (G) Overexpression of miR-491 inhibits cell proliferation in MG63 xenograft models. Tumor tissues from MG63 xenograft model were stained with Ki-67. (H) Apoptotic cells were detected using a TUNEL assay in the indicated xenograft tumor samples. *$p < 0.05$; **$p < 0.01$; ***$p < 0.001$.

Saos-2 cells (Figure S4A). Cells were then analyzed with MTT, apoptosis, and metastasis assays. As expected, exogenously expressed CRYAB blocked the miR-491-mediated inhibition of metastasis (Figure 5A). In addition, the enhanced effect of CDDP on cell growth inhibition mediated by miR-491 was blocked by restoration of CRYAB in Saos-2 cells (Figure 5B). In contrast, knockdown of CRYAB (Figure S4B) blocked the inhibition of miR-491-induced stimulation of OS cell invasion and resistance to CDDP (Figures 5C and 5D). Taken together, these data suggest that CRYAB is an important player in the effects of miR-491 on OS cell metastasis and chemoresistance.

## DISCUSSION

The identification of prognostic factors that can stratify patients according to clinical and biological markers may help to select adequate treatment strategies.[23] Serum is an ideal biological sample that is easy to collect and contains an archive of information because of the

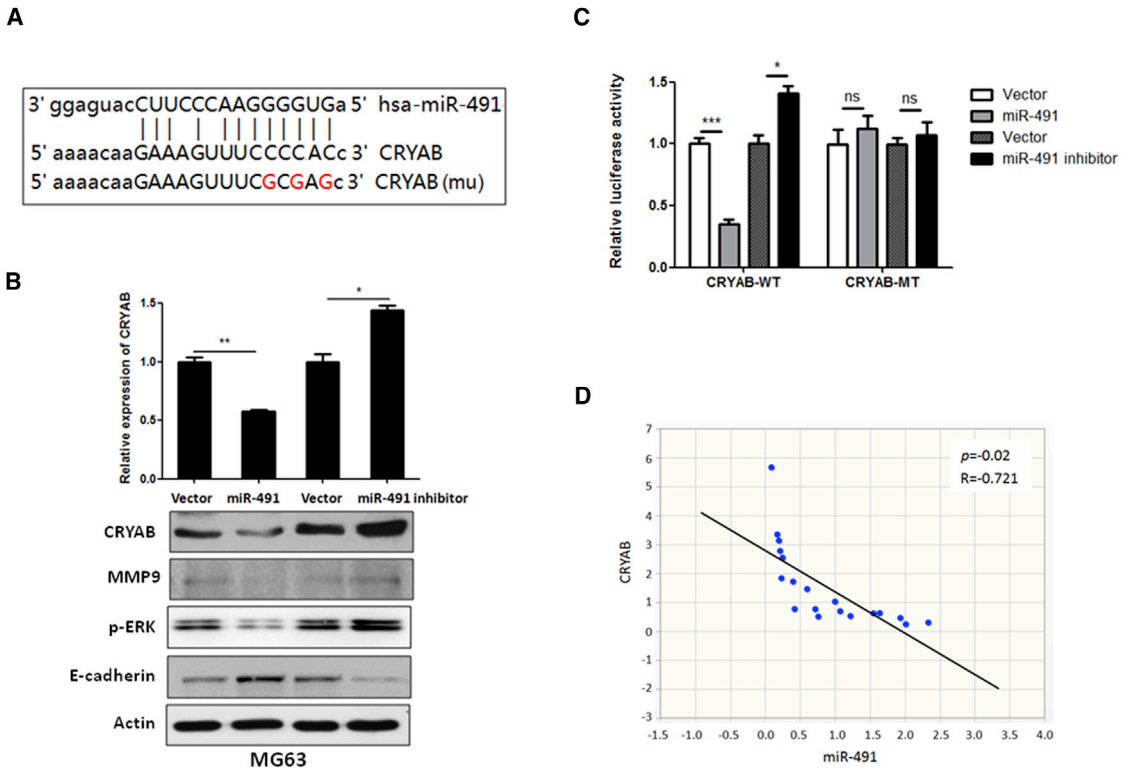


**Figure 4. CRYAB Is a Target of miR-491 in OS**

(A) Sequence alignment of miR-491 with the 3′ UTR of CRYAB genes. (B) miR-491 negatively regulates CRYAB expression and its downstream signaling. MG63 cells that stably express miR-491 or miR-491-antisense were subjected to qRT-PCR and western blot analysis. (C) A 3′ UTR luciferase reporter assay for CRYAB. Wild-type (CRYAB-WT) or mutant 3′ UTR of CRYAB (CRYAB-MT) luciferase reporter constructs were transfected into MG63 cells that stably express miR-491 or miR-491-antisense. After 48 hr of transfection, the luciferase intensity was assessed. (D) The expression of miR-491 and CRYAB was inversely correlated in OS specimens. Using qRT-PCR, we analyzed the expression of miR-491 and CRYAB mRNA in human OS samples (n = 19). *p < 0.05; **p < 0.01; ***p < 0.001.

presence of a variety of DNA, RNA, and proteins released by tissues.[24] However, not every miRNA that is abnormally expressed in tumor tissues is reflected in the serum. Here, we provide the first evidence that miR-491 was indeed downregulated in the serum of OS patients compared with healthy controls. Notably, we found that a decreased level of serum miR-491 was significantly correlated with increased metastasis and a poor chemoresponse in OS patients. Metastasis and chemoresistance are important prognostic factors and are associated with poor survival in patients with OS.[5,25] In fact, our Kaplan-Meier survival analysis revealed that patients with OS whose serum displayed a low expression level of miR-491 had short overall survival. In addition, our multivariate analysis indicates that serum miR-491 level is an independent prognostic factor for OS patient survival. Taken together, these findings suggest that serum level of miR-491 has potential as a biomarker for predicting OS progression and prognosis of OS patients.

Treatment of OS patients often fails because of development of metastasis and chemoresistance.[5,25] In this study, we performed a series of in vitro and in vivo experiments to provide evidence that decreased expression of miR-491 significantly contributes to lung metastasis and chemoresistance through inhibition of apoptosis in OS. Studies show that defects in apoptosis are implicated in the progression of virtually all types of human cancers, including OS.[26,27] Thus, one strategy for cancer treatment is the induction of apoptosis. In fact, accumulating evidence shows that induction of apoptosis can dramatically suppress tumor growth, chemoresistance, and metastasis.[28] Our data clearly show that overexpression of miR-491 can significantly enhance CDDP-induced apoptosis of OS cells, and it dramatically inhibits OS cell metastasis in vitro and in vivo, suggesting that restoration of miR-491 may be a useful strategy for treatment of lung metastasis and chemoresistance in OS patients.

In this study, we also clarified the tumor inhibition mechanism of miR-491 in OS. A previous in vitro study showed that miR-491 inhibits cell migration by directly targeting FOXP4 in OS cells.[21] However, our clinical data show that there is no correlation between the expression of miR-491 and FOXP4 in OS specimens, suggesting that FOXP4 is not a major target gene of miR-491 in OS. In this study, we identified CRYAB as a novel target gene of miR-491 on OS cells. CRYAB is an oncogene. The expression of CRYAB is significantly increased in OS tissues, and elevated expression of CRYAB was

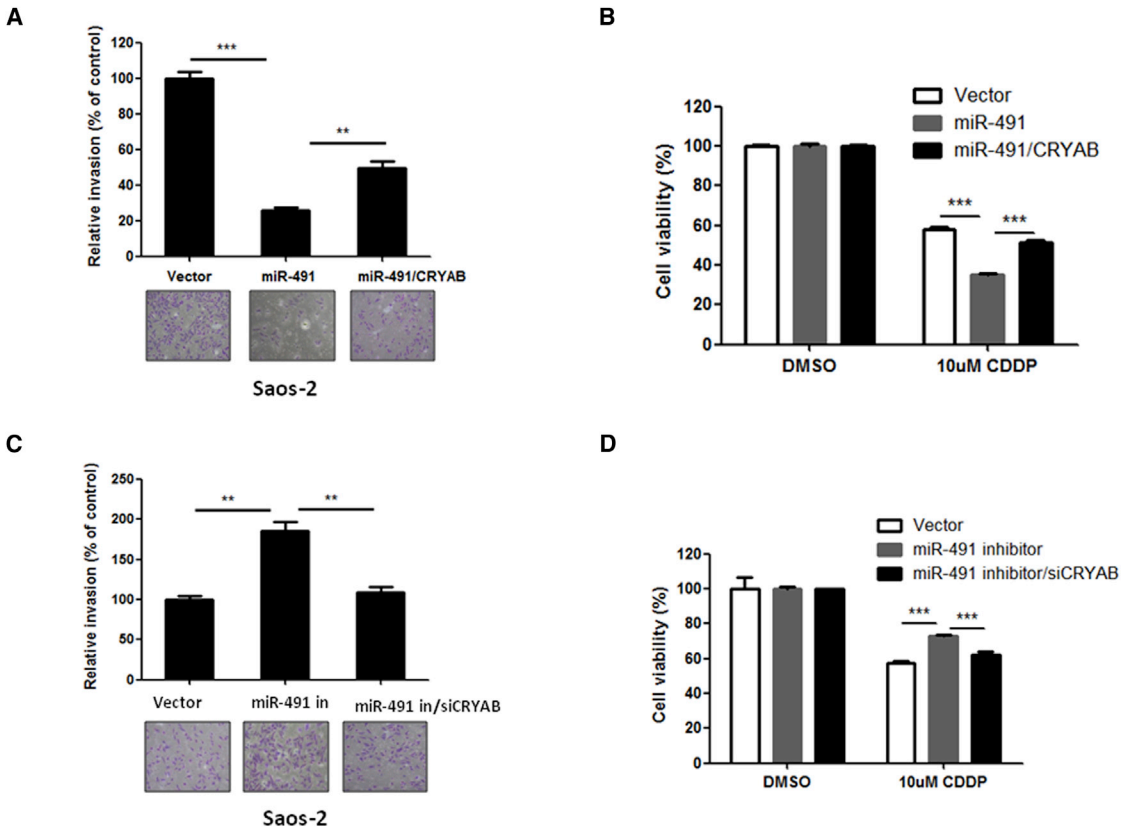


**Figure 5. Effects of miR-491 on OS Cell Metastasis and Sensitivity to CDDP Are Mediated through CRYAB**

(A) Restoration of CRYAB blocked inhibition of OS cell invasion by miR-491. Saos-2 cells stably expressing miR-491 were transfected with a CRYAB expression plasmid for 24 hr and then subjected to a Transwell assay. (B) Restoration of CRYAB protected cells from combination treatment with miR-491 and CDDP. Saos-2 cells stably expressing miR-491 were transfected with a CRYAB expression plasmid. After 24 hr of transfection, cells were incubated with or without CDDP for 48 hr and then subjected to an MTT assay. (C) Silencing of CRYAB blocked stimulation of cell invasion induced by miR-491 inhibition. Saos-2 cells stably expressing miR-491-antisense were transfected with an siRNA of CRYAB (siCRYAB) for 24 hr and then subjected to a Transwell assay. (D) Silencing of CRYAB inhibited CDDP resistance in OS cells induced by miR-491 inhibition. Saos-2 cells that stably expressed miR-491-antisense were transfected with siCRYAB. After 24 hr of transfection, cells were incubated with or without CDDP for 48 hr and then subjected to an MTT assay. $^{**}p < 0.01$; $^{***}p < 0.001$.

positively correlated with metastasis, poor chemoresponse, and shortened survival time in OS patients.[9] Here, our data show that the restoration of miR-491 expression in OS cells leads to the suppression of CRYAB expression; conversely, inhibition of miR-491 further upregulates CRYAB expression. Luciferase reporter gene experiments show that miR-491 directly targets the 3′ UTR of CRYAB. In addition, our clinical data show that expression of CRYAB is inversely correlated with miR-491 in OS specimens. Furthermore, our data indicate that restoration of CRYAB blocked the miR-491 overexpression-induced inhibition of OS cell metastasis and chemosensitivity. These findings clearly suggest that increased expression of CRYAB is partially caused by decreased expression miR-491, and CRYAB is a key downstream effector that mediates the effects of miR-491 on OS cell metastasis and chemoresistance.

In summary, we combined clinical and experimental studies to determine the clinical significance and the role of miR-491 in the progression of OS. Our findings suggest that downregulation of miR-491 is significantly associated with OS progression. Our findings may also aid in the development of potential therapeutics for the treatment of OS lung metastasis and chemoresistance.

## MATERIALS AND METHODS

### Reagents

Fetal bovine serum (FBS), MTT, glutaraldehyde, puromycin, CDDP, anti-actin antibody, and cell culture medium were purchased from Sigma. The small interfering RNA (siRNA) for αB-cryab (CRYAB), QuantiTect SYBR Green PCR Kit, and miRNeasy Serum/Plasma Kit were obtained from QIAGEN. An miR-491-antisense expression vector and CRYAB expression plasmid were from GeneCopoeia. CRYAB antibody was obtained from Novus Biologicals. Antibodies against Ki-67, p-ERK (Thr202/Tyr204), E-cadherin, and MMP-9 were purchased from Cell Signaling Technologies. A Dual-Luciferase Assay Kit and Lipofectamine 2000 were obtained from Promega. TRIzol and a BLOCK-iT Pol II miR RNAi Expression Vector Kit were purchased from Invitrogen. Opti-MEM, a High-Capacity

**Table 3. Characteristics of Patients with OS**

| Variables | Healthy Control Subjects | No. of Patients (%) miR-491 Low (n = 58) | miR-491 High (n = 44) | p Value |
|---|---|---|---|---|
| Gender | | | | 0.50 |
| Male | 8 | 32 (55.17) | 22 (50.00) | |
| Female | 12 | 26 (44.83) | 22 (50.00) | |
| Age | | | | |
| Median | 24.5 | 17.3 | 16.4 | |
| Range | 7–43 | 4–41 | 4–40 | |
| Anatomical site | | | | 0.88 |
| Femur | | 29 (50.00) | 23 (52.27) | |
| Tibia | | 13 (22.41) | 12 (27.27) | |
| Humerus | | 12 (20.69) | 6 (13.64) | |
| Pelvis | | 2 (3.45) | 1 (2.27) | |
| Other | | 2 (3.45) | 2 (4.55) | |
| Histologic subtype | | | | 0.63 |
| Osteoblastic | | 33 (56.90) | 27 (61.36) | |
| Chondroblastic | | 7 (12.07) | 6 (13.64) | |
| Fibroblastic | | 13 (22.41) | 5 (11.36) | |
| Telangiectatic | | 3 (5.17) | 3 (6.82) | |
| Other | | 2 (3.45) | 3 (6.82) | |
| Histologic grade | | | | 0.18 |
| III | | 8 (13.79) | 2 (4.55) | |
| IV | | 50 (86.21) | 42 (95.45) | |
| Enneking grade | | | | 0.77 |
| 2A | | 9 (15.52) | 5 (11.36) | |
| 2B | | 49 (84.48) | 39 (88.64) | |

cDNA Reverse Transcription Kit, an miRNA expression reporter vector, miR-491 mimics, antisense oligonucleotides of miR-491 (ASO miR-491), negative control oligonucleotides (NC), and an miR-491 primer set were purchased from Life Technologies. EDTA-containing Vacutainer tubes and Invasion Assay Kits were obtained from BD Biosciences. An apoptosis assay kit and an In Situ Cell Death Detection kit were purchased from Biotium and Roche, respectively.

### Cell Culture and Human Samples

The OS cell lines MG63, Saos-2, and U2OS were obtained from the American Type Culture Collection, and 143B was obtained from the Type Culture Collection of the Chinese Academy of Sciences. All cells were cultured in DMEM, supplemented with 10% FBS, at 37°C in an atmosphere of 95% air and 5% $CO_2$.

Blood and tumor samples were collected from 102 patients with newly diagnosed OS (no metastasis at diagnosis) at the General Hospital of the People's Liberation Army. None of the patients had received preoperative adjuvant chemotherapy before the blood was drawn. Blood samples were also obtained from 20 healthy individuals. Blood samples were allowed to stand for 30 min and then were centrifuged at 1,000 × *g* for 15 min in 4°C. The supernatant sera were recovered and stored at −80°C until analysis. For evaluation of the chemotherapy response, OS specimens were also obtained at resection after chemotherapy. The characteristics of the OS patients and healthy controls are summarized in Table 3. This research was approved by the Research Ethics Board of the General Hospital of the People's Liberation Army.

### Histological Response Evaluation

All patients received the same multidrug chemotherapy regimen as described previously.[29] The histological response was reviewed by an expert panel of pathologists. When the percentage of tumor necrosis was ≥90%, the patients were classified as good responders, and when the percentage of tumor necrosis was lower than 90%, the patients were defined as poor responders.[30]

### Real-Time qRT-PCR Analysis

Total RNA was isolated from cells and tissues using TRIzol reagent according to the manufacturer's protocol. miRNAs from serum were isolated using the miRNeasy Serum/Plasma Kit following the manufacturer's instructions. Mature miR-491 and the RNU6 endogenous control were analyzed using the TaqMan microRNA Assay Kit. The expression of miR-491 was quantified in relation to the expression of RNU6. For analysis of CRYAB expression, RT and PCR were performed with a High-Capacity cDNA Reverse Transcription Kit and QuantiTect SYBR Green PCR kit, respectively. The expression of CRYAB was quantified in relation to the expression of β-actin. Primers for CRYAB were 5′-CTTTGACCAGTTCTTCG GAG-3′ and 5′-TCCGTGTTCAGCTGCTGGTA-3′; primers for β-actin were 5′-AGAGCTACGAGCTGCC TGAC-3′ and 5′-AGC ACTGTGTTGGCGTACAG-3′.

### Luciferase Reporter Assay

In brief, 3′ UTR segments of CRYAB that were predicted to interact with miR-491 were amplified by PCR from human genomic DNA and inserted into the *Mlu I* and *Hind III* sites of the miRNA Expression Reporter Vector. For the luciferase reporter experiments, the indicated cells were seeded into 24-well cell culture plates at a concentration of $1 \times 10^4$ per well. On the next day, the cells were transfected with the indicated reporter plasmids containing firefly luciferase. The Renilla luciferase plasmid was cotransfected as a transfection control. Cells were lysed 48 hr after transfection, and luciferase activity was measured by a Dual-Luciferase Assay System according to the manufacturer's protocol. The firefly luciferase activity was normalized by the activity of Renilla luciferase.

### Western Blot and Immunohistochemistry Assays

Western blotting and immunohistochemical assays were performed as described previously.[31]

### MTT and Apoptosis Analysis

For the MTT assay, cells were transfected with the indicated oligonucleotides or plasmid using Lipofectamine 2000. After 24 hr of

transfection, cells were plated into 96-well plates at a density of $5 \times 10^3$ cells per well. After 12 hr of seeding, cells were incubated with or without 10 μM CDDP for 48 hr. The cell viability was measured using MTT according to the manufacturer's protocol.

For apoptosis analysis, cells were seeded in six-well plates after 24 hr of transfection; then cells were incubated with the indicated drugs. After 24 hr, cells were harvested and stained with annexin V and 7-aminoactinomycin D (7-AAD) according to the manufacturer's protocol, followed by flow cytometric analysis. The apoptotic cells in tumor tissues were detected using an In Situ Cell Death Detection kit according to the manufacturer's instructions.

### Invasion Assay

Cells were transfected with the indicated oligonucleotides or plasmid for 24 hr; then $1 \times 10^4$ cells in growth medium without serum were seeded in the upper wells of BD Chambers. The lower wells contained the same medium with 10% serum. After 24 hr, the cells that had invaded to the lower side of the chamber were fixed with 2.5% glutaraldehyde, stained with 0.1% crystal violet, dried, and counted.

### Stable Cell Line Selection

An miR-491 expression vector was constructed using a LOCK-iT Pol II miR RNAi Expression Vector Kit according to the manufacturer's protocol and transfected into the indicated cells for selection of stable miR-491-expressing cells. After 48 hr of transfection, cells were incubated with 10 mg/mL blasticidin for 2 weeks. To construct stably expressing miR-491-antisense cells, we transfected an miR-491-antisense expression vector into the indicated cells. After 48 hr of transfection, cells were incubated with 2 mg/mL puromycin for 1 week. Then, cells were frozen in aliquots for later use.

### Animal Experiments

Stably expressing miR-491 or miR-491-antisense cells and their vector control cells were used to generate the animal model. For the subcutaneous tumor growth assay, $2 \times 10^6$ of the indicated cells in 0.1 mL of PBS were subcutaneously injected into 6-week-old female nude mice (eight mice per group). When tumors reached a size of approximately 100 $mm^3$, the mice were started on a treatment of either PBS or CDDP (10 mg/kg body weight). The treatment was administered every third day. After 3 weeks, the mice were sacrificed, and the tumor weights were measured. For the lung metastasis experiments, we generated OS lung metastatic models by injection of OS cells through the tail vein or the intramedullary cavity of the tibia. For tail vein injection, $5 \times 10^5$ of the indicated cells were suspended in 0.1 mL of PBS and injected into the lateral tail vein of 6-week-old female nude mice (eight mice per group). At 6 weeks after injection, all mice were sacrificed, and the lung surface tumor foci were counted. For tibia intramedullary cavity injection, $5 \times 10^5$ 143B cells in 5 μL of matrigel per mouse were injected into the intramedullary cavity of the tibia as described by Hayashi et al.[32] previously. At 4 weeks after injection, all mice were sacrificed, and the lung surface tumor foci were counted. The mice were obtained from Charles River Laboratory or Shanghai Laboratory Animal Center, and all animal care and experimentation were conducted according to the guidelines of the Institutional Animal Care and Use Committee of the University of South Florida and Third Military Medical University of China.

### Statistical Analysis

All data are presented as the mean ± SD, and significant differences between treatment groups were analyzed by Student's t test or one-way ANOVA and Duncan's multiple range test using SAS statistical software version 6.12 (SAS Institute). The survival rate of patients with non-small-cell lung cancer (NSCLC) was calculated using a Kaplan-Meier survival analysis. The significance of multiple predictors of survival was assessed using Cox regression analysis. Differences were considered statistically significant at $p < 0.05$.

## SUPPLEMENTAL INFORMATION

Supplemental Information includes four figures and can be found with this article online at http://dx.doi.org/10.1016/j.ymthe.2017.05.018.

## AUTHOR CONTRIBUTIONS

H.J. and C.-X.X. designed the experiments and wrote the paper; S.-N.W., S.L., Yun Wang, W. Gou, M.X., H.Z., and Q.L. performed experiments; all authors analyzed data; and C.L., Z.P., Yan Wang, Z.-Z.Y., and D.W. provided reagents.

## CONFLICTS OF INTEREST

There is no conflict of interest to disclose.

## ACKNOWLEDGMENTS

This work was supported by the National Natural Science Foundation of China (grant 81402216 to M.X. and grant 81672657 to C.-X.X.); the Beijing New-star Plan of Science and Technology (grant Z14110700181409 to M.X.); the Natural Science Foundation of Chongqing Science and Technology Commission (grant cstc2313jcyjA10106 to S.-N.W.); and the Startup Fund for Talented Scholars of Daping Hospital and Research Institute of Surgery, Third Military Medical University (to C.-X.X. and H.J.).

## REFERENCES

1. Messerschmitt, P.J., Garcia, R.M., Abdul-Karim, F.W., Greenfield, E.M., and Getty, P.J. (2009). Osteosarcoma. J. Am. Acad. Orthop. Surg. *17*, 515–527.
2. Thayanithy, V., Sarver, A.L., Kartha, R.V., Li, L., Angstadt, A.Y., Breen, M., Steer, C.J., Modiano, J.F., and Subramanian, S. (2012). Perturbation of 14q32 miRNAs-cMYC gene network in osteosarcoma. Bone *50*, 171–181.
3. Broadhead, M.L., Clark, J.C., Myers, D.E., Dass, C.R., and Choong, P.F. (2011). The molecular pathogenesis of osteosarcoma: a review. Sarcoma *2011*, 959248.
4. Marulanda, G.A., Henderson, E.R., Johnson, D.A., Letson, G.D., and Cheong, D. (2008). Orthopedic surgery options for the treatment of primary osteosarcoma. Cancer Contr. *15*, 13–20.
5. Huang, J., Ni, J., Liu, K., Yu, Y., Xie, M., Kang, R., Vernon, P., Cao, L., and Tang, D. (2012). HMGB1 promotes drug resistance in osteosarcoma. Cancer Res. *72*, 230–238.
6. PosthumaDeBoer, J., Witlox, M.A., Kaspers, G.J., and van Royen, B.J. (2011). Molecular alterations as target for therapy in metastatic osteosarcoma: a review of literature. Clin. Exp. Metastasis *28*, 493–503.
7. Huang, X.Y., Ke, A.W., Shi, G.M., Zhang, X., Zhang, C., Shi, Y.H., Wang, X.Y., Ding, Z.B., Xiao, Y.S., Yan, J., et al. (2013). αB-crystallin complexes with 14-3-3ζ to induce

epithelial-mesenchymal transition and resistance to sorafenib in hepatocellular carcinoma. Hepatology *57*, 2235–2247.

8. Kim, H.S., Lee, Y., Lim, Y.A., Kang, H.J., and Kim, L.S. (2011). αB-crystallin is a novel oncoprotein associated with poor prognosis in breast cancer. J. Breast Cancer *14*, 14–19.
9. Shi, Q.M., Luo, J., Wu, K., Yin, M., Gu, Y.R., and Cheng, X.G. (2016). High level of αB-crystallin contributes to the progression of osteosarcoma. Oncotarget *7*, 9007–9016.
10. Zhang, L., Zhang, L., Xia, X., He, S., He, H., and Zhao, W. (2016). Krüppel-like factor 4 promotes human osteosarcoma growth and metastasis via regulating CRYAB expression. Oncotarget *7*, 30990–31000.
11. Kim, V.N. (2005). MicroRNA biogenesis: coordinated cropping and dicing. Nat. Rev. Mol. Cell Biol. *6*, 376–385.
12. Bartel, D.P. (2004). MicroRNAs: genomics, biogenesis, mechanism, and function. Cell *116*, 281–297.
13. Wang, R.T., Xu, M., Xu, C.X., Song, Z.G., and Jin, H. (2014). Decreased expression of miR216a contributes to non-small-cell lung cancer progression. Clin. Cancer Res. *20*, 4705–4716.
14. Xu, M., Jin, H., Xu, C.X., Sun, B., Mao, Z., Bi, W.Z., and Wang, Y. (2014). miR-382 inhibits tumor growth and enhance chemosensitivity in osteosarcoma. Oncotarget *5*, 9472–9483.
15. Xu, M., Jin, H., Xu, C.X., Sun, B., Song, Z.G., Bi, W.Z., and Wang, Y. (2015). miR-382 inhibits osteosarcoma metastasis and relapse by targeting Y box-binding protein 1. Mol. Ther. *23*, 89–98.
16. Samaeekia, R., Adorno-Cruz, V., Bockhorn, J., Chang, Y.F., Huang, S., Prat, A., Ha, N., Kibria, G., Huo, D., Zheng, H., et al. (2017). miR-206 inhibits stemness and metastasis of breast cancer by targeting MKL1/IL11 pathway. Clin. Cancer Res. *23*, 1091–1103.
17. Ryu, S., McDonnell, K., Choi, H., Gao, D., Hahn, M., Joshi, N., Park, S.M., Catena, R., Do, Y., Brazin, J., et al. (2013). Suppression of miRNA-708 by polycomb group promotes metastases by calcium-induced cell migration. Cancer Cell *23*, 63–76.
18. Gasparini, P., Cascione, L., Landi, L., Carasi, S., Lovat, F., Tibaldi, C., Alì, G., D'Incecco, A., Minuti, G., Chella, A., et al. (2015). microRNA classifiers are powerful diagnostic/prognostic tools in ALK-, EGFR-, and KRAS-driven lung cancers. Proc. Natl. Acad. Sci. USA *112*, 14924–14929.
19. Marchini, S., Cavalieri, D., Fruscio, R., Calura, E., Garavaglia, D., Fuso Nerini, I., Mangioni, C., Cattoretti, G., Clivio, L., Beltrame, L., et al. (2011). Association between miR-200c and the survival of patients with stage I epithelial ovarian cancer: a retrospective study of two independent tumour tissue collections. Lancet Oncol. *12*, 273–285.
20. Imaoka, H., Toiyama, Y., Fujikawa, H., Hiro, J., Saigusa, S., Tanaka, K., Inoue, Y., Mohri, Y., Mori, T., Kato, T., et al. (2016). Circulating microRNA-1290 as a novel diagnostic and prognostic biomarker in human colorectal cancer. Ann. Oncol. *27*, 1879–1886.
21. Yin, Z., Ding, H., He, E., Chen, J., and Li, M. (2017). Up-regulation of microRNA-491-5p suppresses cell proliferation and promotes apoptosis by targeting FOXP4 in human osteosarcoma. Cell Prolif. *50*, e12308.
22. Huang, W.C., Chan, S.H., Jang, T.H., Chang, J.W., Ko, Y.C., Yen, T.C., Chiang, S.L., Chiang, W.F., Shieh, T.Y., Liao, C.T., et al. (2014). miRNA-491-5p and GIT1 serve as modulators and biomarkers for oral squamous cell carcinoma invasion and metastasis. Cancer Res. *74*, 751–764.
23. Le, N., Sund, M., and Vinci, A.; GEMS collaborating group of Pancreas 2000 (2016). Prognostic and predictive markers in pancreatic adenocarcinoma. Dig. Liver Dis. *48*, 223–230.
24. Tian, F., Shen, Y., Chen, Z., Li, R., Lu, J., and Ge, Q. (2016). Aberrant miR-181b-5p and miR-486-5p expression in serum and tissue of non-small cell lung cancer. Gene *591*, 338–343.
25. Bielack, S.S., Kempf-Bielack, B., Branscheid, D., Carrle, D., Friedel, G., Helmke, K., Kevric, M., Jundt, G., Kühne, T., Maas, R., et al. (2009). Second and subsequent recurrences of osteosarcoma: presentation, treatment, and outcomes of 249 consecutive cooperative osteosarcoma study group patients. J. Clin. Oncol. *27*, 557–565.
26. Li, J., Yang, Z., Li, Y., Xia, J., Li, D., Li, H., Ren, M., Liao, Y., Yu, S., Chen, Y., et al. (2016). Cell apoptosis, autophagy and necroptosis in osteosarcoma treatment. Oncotarget *7*, 44763–44778.
27. Shivapurkar, N., Reddy, J., Chaudhary, P.M., and Gazdar, A.F. (2003). Apoptosis and lung cancer: a review. J. Cell. Biochem. *88*, 885–898.
28. Symonds, H., Krall, L., Remington, L., Saenz-Robles, M., Lowe, S., Jacks, T., and Van Dyke, T. (1994). p53-dependent apoptosis suppresses tumor growth and progression in vivo. Cell *78*, 703–711.
29. Xu, M., Xu, C.X., Bi, W.Z., Song, Z.G., Jia, J.P., Chai, W., Zhang, L.H., and Wang, Y. (2013). Effects of endostar combined multidrug chemotherapy in osteosarcoma. Bone *57*, 111–115.
30. Ferrari, S., Smeland, S., Mercuri, M., Bertoni, F., Longhi, A., Ruggieri, P., Alvegard, T.A., Picci, P., Capanna, R., Bernini, G., et al.; Italian and Scandinavian Sarcoma Groups (2005). Neoadjuvant chemotherapy with high-dose Ifosfamide, high-dose methotrexate, cisplatin, and doxorubicin for patients with localized osteosarcoma of the extremity: a joint study by the Italian and Scandinavian Sarcoma Groups. J. Clin. Oncol. *23*, 8845–8852.
31. Xu, C.X., Jere, D., Jin, H., Chang, S.H., Chung, Y.S., Shin, J.Y., Kim, J.E., Park, S.J., Lee, Y.H., Chae, C.H., et al. (2008). Poly(ester amine)-mediated, aerosol-delivered Akt1 small interfering RNA suppresses lung tumorigenesis. Am. J. Respir. Crit. Care Med. *178*, 60–73.
32. Hayashi, K., Zhao, M., Yamauchi, K., Yamamoto, N., Tsuchiya, H., Tomita, K., Kishimoto, H., Bouvet, M., and Hoffman, R.M. (2009). Systemic targeting of primary bone tumor and lung metastasis of high-grade osteosarcoma in nude mice with a tumor-selective strain of Salmonella typhimurium. Cell Cycle *8*, 870–875.

**YMTHE, Volume *25***

## Supplemental Information

# miR-491 Inhibits Osteosarcoma Lung Metastasis and Chemoresistance by Targeting αB-crystallin

**Shu-Nan Wang, Song Luo, Chang Liu, Zhenghao Piao, Wenlong Gou, Yun Wang, Wei Guan, Qing Li, Hua Zou, Zhen-Zhou Yang, Dong Wang, Yan Wang, Meng Xu, Hua Jin, and Cheng-Xiong Xu**

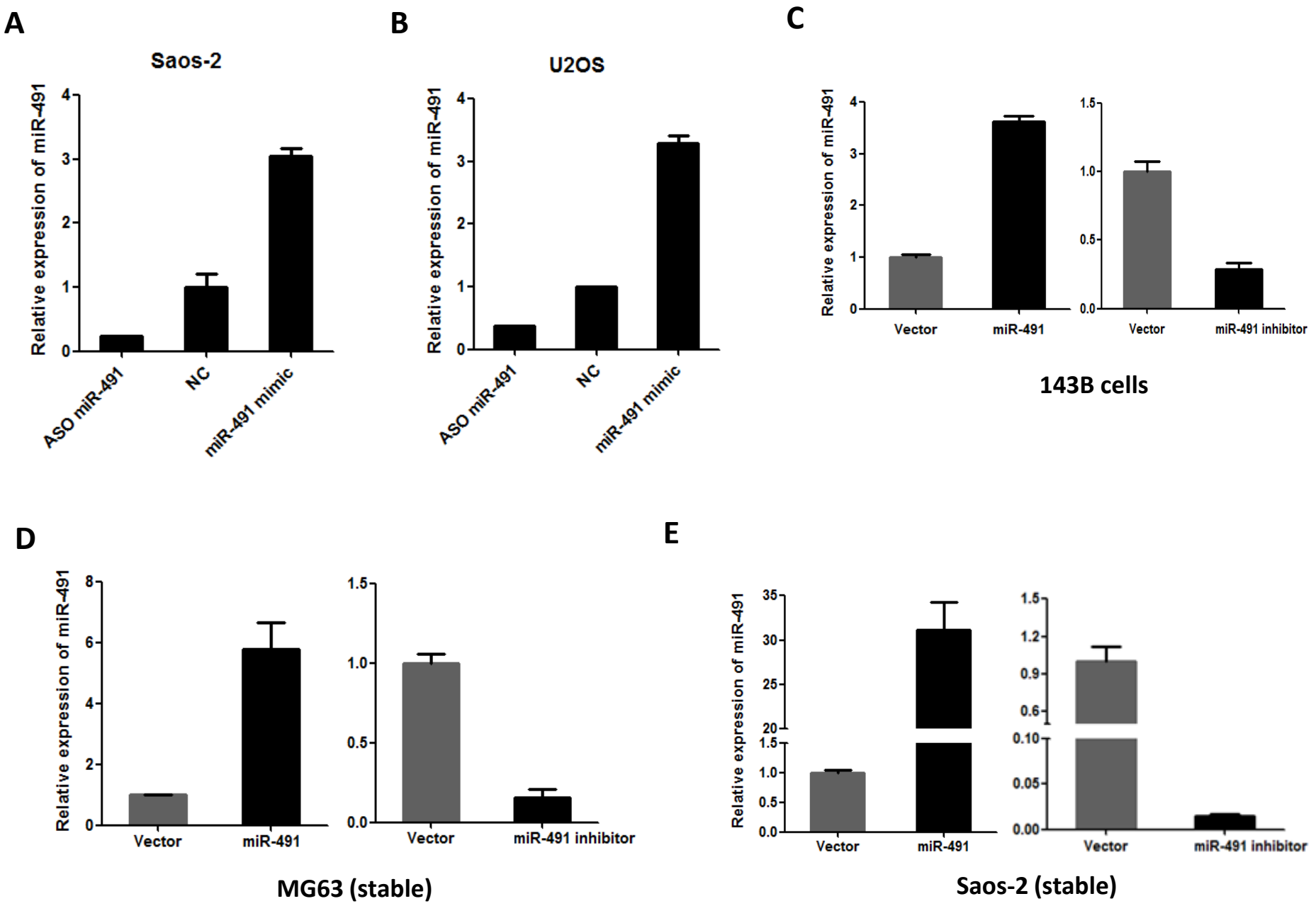
A
Saos-2
Relative expression of miR-491
ASO miR-491
NC
miR-491 mimic
B
U2OS
Relative expression of miR-491
ASO miR-491
NC
miR-491 mimic
C
Relative expression of miR-491
Vector
miR-491
Vector
miR-491 inhibitor
143B cells
D
Relative expression of miR-491
Vector
miR-491
Vector
miR-491 inhibitor
MG63 (stable)
E
Relative expression of miR-491
Vector
miR-491
Vector
miR-491 inhibitor
Saos-2 (stable)

Figure S1

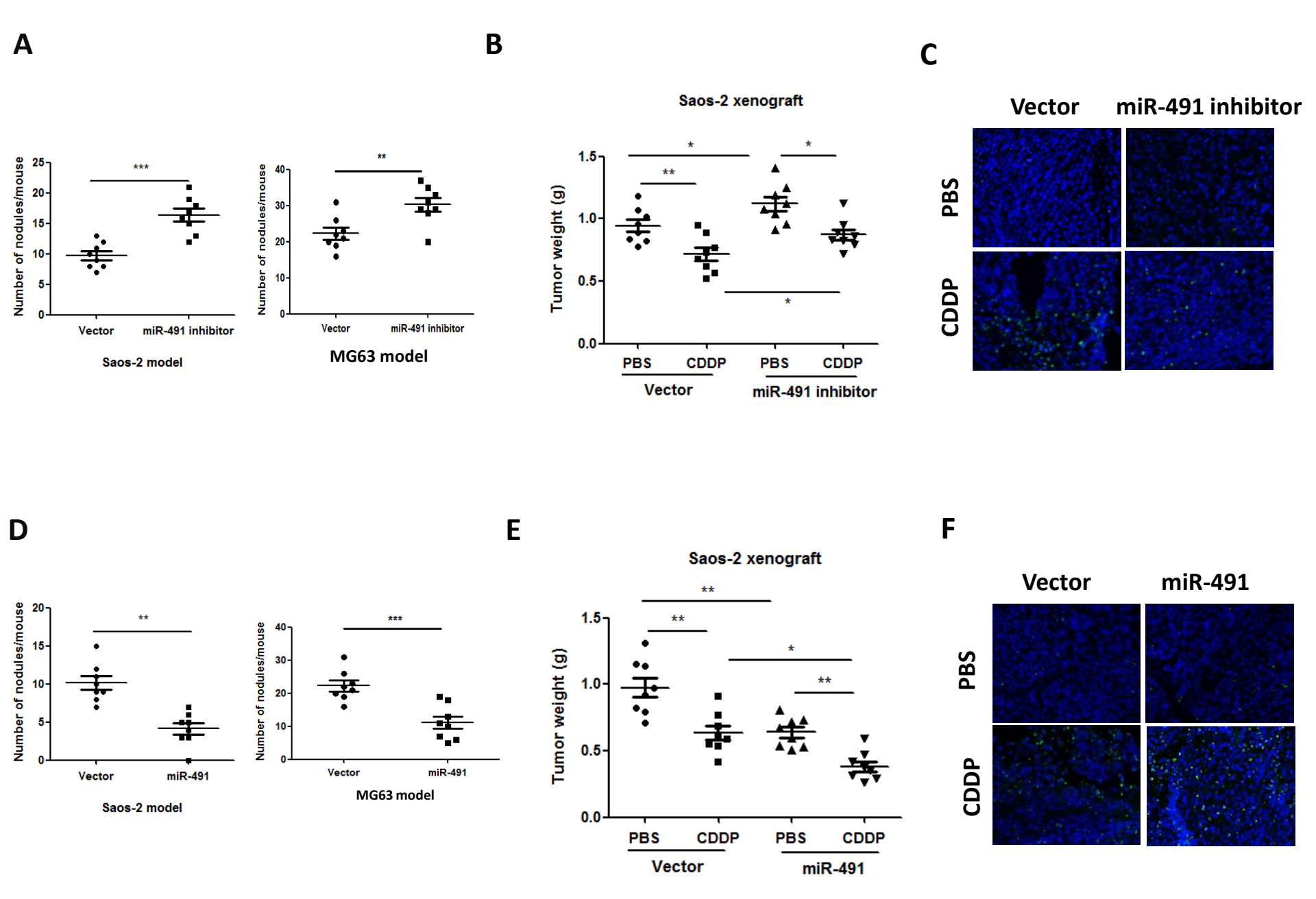
A
Number of nodules/mouse
***
Vector
miR-491 inhibitor
Saos-2 model
**
MG63 model
B
Saos-2 xenograft
Tumor weight (g)
PBS
CDDP
Vector
miR-491 inhibitor
C
Vector
miR-491 inhibitor
PBS
CDDP
D
**
***
miR-491
E
miR-491
F

Figure S2.

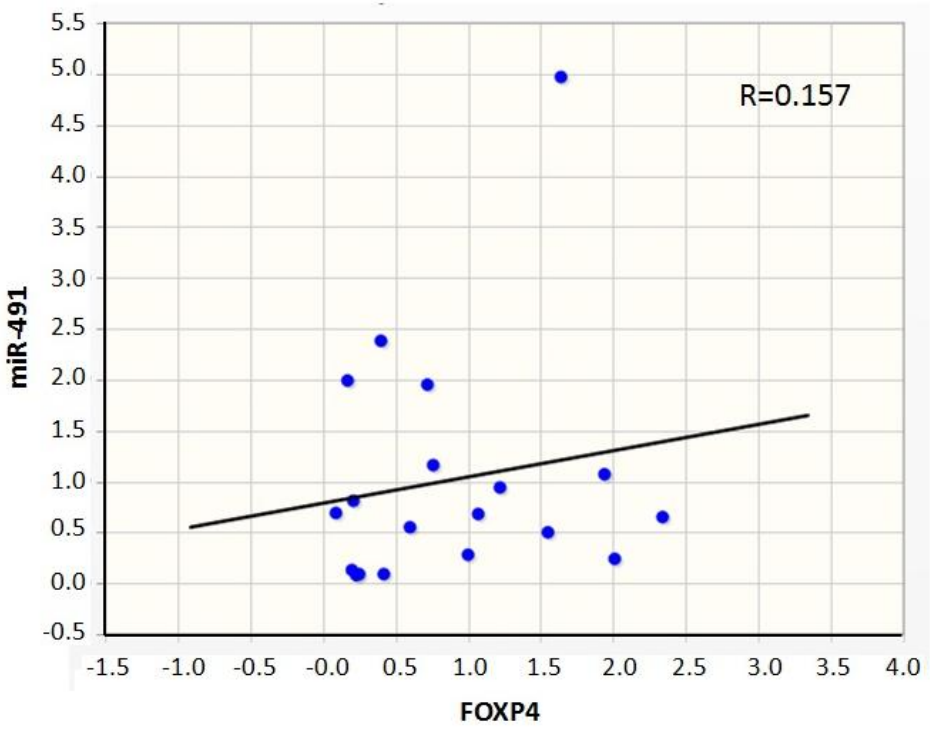
R=0.157
miR-491
FOXP4
5.5
5.0
4.5
4.0
3.5
3.0
2.5
2.0
1.5
1.0
0.5
0.0
-0.5
-1.5
-1.0
-0.5
-0.0
0.5
1.0
1.5
2.0
2.5
3.0
3.5
4.0

**Figure S3.**

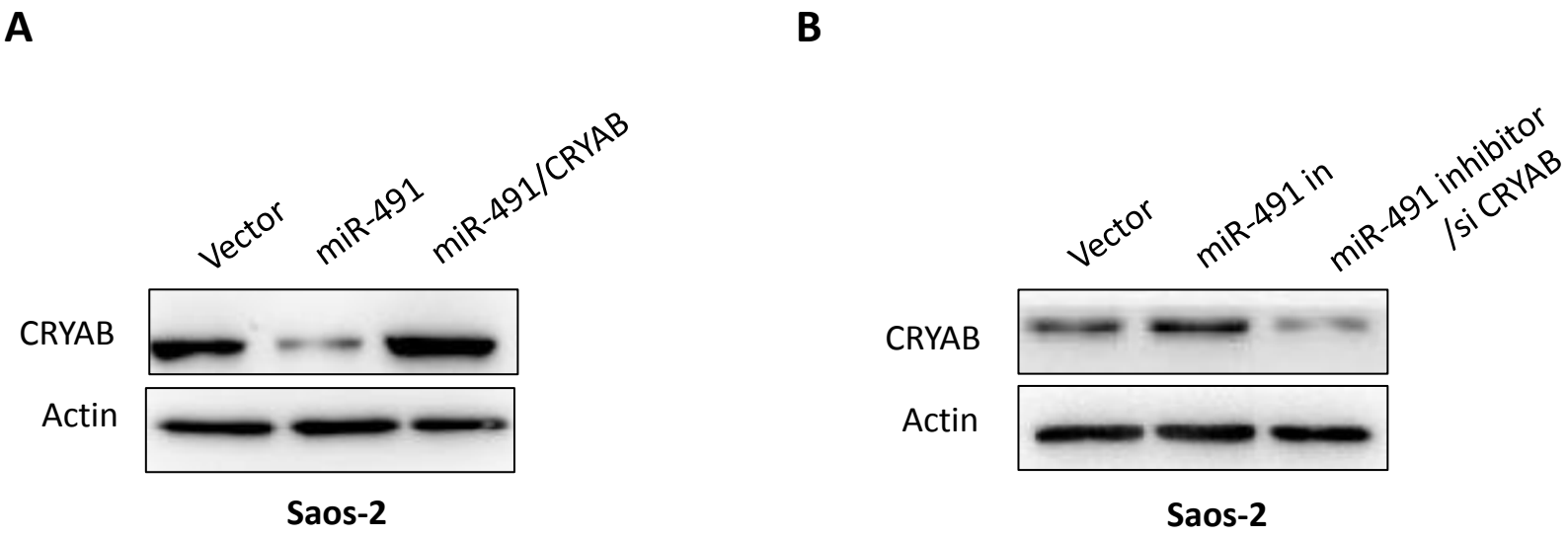
A
Vector
miR-491
miR-491/CRYAB
CRYAB
Actin
Saos-2
B
Vector
miR-491 in
miR-491 inhibitor /si CRYAB
CRYAB
Actin
Saos-2

**Figure S4.**

## SUPPLEMENTARY FIGURE LEGENDS

**Figure S1. Expression of miR-491 in indicated OS cells.** (A) Saos-2 cells were transfected with the indicated oligonucleotides. After 48 hours of transfection, the cells were subjected to RT-qPCR analysis to detect the miR-491 expression level. (B) U2OS cells were transfected with the indicated oligonucleotides. After 48 hours of transfection, the cells were subjected to RT-qPCR analysis to detect the miR-491 expression level. (C) 143B cells were transfected with the indicated plasmids. After 72 hours of transfection, the cells were subjected to RT-qPCR analysis to detect the miR-491 expression level. (D) The expression level of miR-491 was measured by RT-qPCR in Saos-2 cells stably expressing miR-491 (miR-491) or miR-491-antisense (miR-491 inhibitor). (E) the expression level of miR-491 was measured by RT-qPCR in MG63 cells stably expressing miR-491 or miR-491-antisense. NC: negative control oligonucleotides, ASO miR-491: antisense oligonucleotides of miR-491.

**Figure S2. miR-491 negatively regulates OS cell lung metastasis and chemoresistance *in vivo*.** (A) Inhibition of miR-491 stimulates OS cell lung metastasis in an animal model. Indicated cells that stably expressed miR-491-antisense (miR-491 inhibitor) were injected into the tail vein of 6-week-old nude mice (n = 8 per mice). The mice were sacrificed 6 weeks after the tail vein injection, and the lung surface nodules were counted using microscopy. (B) Inhibition of miR-491 promotes tumor growth and induces resistance to CDDP in Saos-2 xenograft models. Saos-2 cells stably expressing miR-491-antisense were injected subcutaneously into nude mice (n = 8 per group). After the tumor size reached approximately 100 $mm^3$, the mice were started on a treatment of either PBS or CDDP (10 mg/kg body weight). The mice were sacrificed after 3 weeks of CDDP treatment, and the tumor weight was measured. (C) Apoptotic cells were detected using a TUNEL assay in the indicated xenograft tumor samples. (D) Overexpression of miR-491 inhibits OS cell lung metastasis. Indicated cells that stably expressed miR-491 (miR-491) were injected into the tail vein of 6-week-old nude mice (*n* = 8

per group). The mice were sacrificed 6 weeks after the tail vein injection, and the lung surface nodules were counted using microscopy. (E) Overexpression of miR-491 inhibits tumor growth and enhances the tumor growth inhibition effect of CDDP in animal models. Saos-2 cells stably expressing miR-491 were injected subcutaneously into nude mice ($n$ = 8 per group). After the tumor size reached approximately 100 $mm^3$, the mice were started on a treatment of either PBS or CDDP (10 mg/kg body weight). The mice were sacrificed after 3 weeks of CDDP treatment, and the tumor weight was measured. F, Apoptotic cells were detected using a TUNEL assay in the indicated xenograft tumor samples.

**Figure S3. Correlation between miR-491 and FOXP4 expression in OS specimens.** Using RT-qPCR, we analyzed the expression of miR-491 and FOXP4 in 18 tumor specimens from patients with OS.

**Figure S4. Expression of CRYAB.** (A) Saos-2 cells that stably overexpressed miR-491 were transfected with a CRYAB expression plasmid. After 72 hours of transfection, cells were subjected to Western blot analysis. (B) Stably overexpressing miR-491-antisense Saos-2 cells were transfected with CRYAB siRNA (siCRYAB). After 72 hours of transfection, cells were subjected to Western blot analysis.